ANTHROPOLOGIE • XXXVIII/2 • pp. 193–200 • 2000

DOUGLAS H. UBELAKER, ERICA B. JONES, HELEN D. DONOGHUE, MARK SPIGELMAN

SKELETAL AND MOLECULAR EVIDENCE FOR TUBERCULOSIS IN A FORENSIC CASE

ABSTRACT: Analysis of a human skeleton submitted as a forensic case from the American Southwest detected skeletal lesions suggestive of tuberculosis. Molecular analysis, using the polymerase chain reaction, of samples removed from these lesions confirmed the presence of DNA specific for Mycobacterium tuberculosis. *Radiocarbon analysis suggests the skeleton is recent but likely dates prior to 1956 AD. This represents the first use of molecular techniques to identify a disease organism in a human skeletonized forensic case and illustrates the potential of this approach for more general forensic analysis. The many sites of bone involvement display the diversity of lesions present within an individual with documented tuberculosis.*

KEY WORDS: Tuberculosis – PCR – Molecular – Skeletal – Forensic

Considerable anthropological attention has focused on tuberculosis, largely because of its skeletal manifestations, great human impact, and its considerable antiquity in both the Old and New Worlds. Research has succeeded in documenting not only an early presence of this disease, but aspects of its population impact as well (Buikstra 1981, Hrdlička 1909).

Althrough evidence of tuberculosis can be found in mummified soft tissue (Allison *et al.* 1973, Aufderheide, Rodríguez-Martín 1998, Dalton *et al.* 1976), it is more often suggested from skeletal lesions due to the greater preservation of bone. The literature suggests that between 5 and 7 percent of tuberculosis cases in the pre-antibiotic era involved bone. The figure is as low as only 1 percent in modern times (Aufderheide, Rodríguez-Martín 1998). Kelley and Micozzi (1984) suggest that the percentage climbs to around 16 when rib lesions are considered. They argue that some rib lesions can be generated directly from the lungs or pleura of persons with pulmonary tuberculosis. Other skeletal manifestations result from the hemotogenous spread of tubercle bacilli. In such cases, the bacilli travel through blood circulation to skeletal areas of cancellous bone and hematopoietic marrow. This process leads to the formation of sequestra of cancellous bone with focal destruction, cavitation, and minimal reactive bone formation.

Authorities agree that the skeletal manifestations of tuberculosis can vary considerably but present some predictable characteristics. Because the tubercle bacilli are distributed by blood, the resulting lesions are most commonly found in areas of greater blood content, such as the metaphysis area of long bones, vertebral centra, and the ilium. Aufderheide and Rodríguez-Martín (1998) report that, in adults, the most common area for skeletal lesions is the joints (90 percent), while 40 percent of lesions are visible in the spinal column. Lesions in the ribs also frequently occur. Other, less common sites, are the flat pelvic bones, long bone diaphysis, sternum and the skull.

Skeletal manifestations of tuberculosis typically involve roughly circular areas of lytic destruction with resulting cavitation. Minimal perifocal reactive bone formation is present, although the involved bone may show perifocal or generalized osteoporosis. Some osteosclerosis is usually present, especially in surrounding trabeculae. The lesions are usually smooth walled and some moderate periosteal reactive bone may be present. Vertebral involvement is usually in the centra rather than the neural arches,

transverse processes, or spinous processes (Aufderheide, Rodríguez-Martín 1998, Kelley *et al.* 1994, Ortner, Putschar 1981, Steinbock 1976).

Vertebral involvement usually concentrates in the lower spine, from the eighth thoracic to the fourth lumbar. When the vertebrae collapse, due to the extent of destruction of the centra, the vertebrae cannot support the weight of the individual, producing angular kyphosis (advanced Pott's disease or gibbus). Aufderheide and Rodríguez-Martín (1998), consider this condition to be the most diagnostic feature of skeletal tuberculosis.

As noted by Aufderheide and Rodriguez-Martin (1998), many other conditions can present evidence similar to aspects of tuberculosis. Examples include chronic pyogenic osteomyelitis, brucella osteomyelitis, fungal infections (such as blastomycosis, or more likely, coccidioidomycosis, given the location of the discovery of the remains in the American Southwest), typhoid spine, healed vertebral fractures, actinomycosis, echinocciasis, histoplasmosis, histiocystosis-X, sarcoidosis, septic arthritis, traumatic arthritis, malignant bone tumours, rheumatoid arthritis, Paget's disease, ankylosing spondylitis, and Scheuermann's disease. They note that even the characteristic Pott's disease has been found in association with *Blastomyces dermatitidis* and *Coccidioides immitis*.

Working largely with skeletal materials, palaeopathologists have for many years attempted to detect evidence for tuberculosis from archaeologically recovered human samples. Many specimens have been proffered from both the Old and New Worlds as displaying characteristics suggestive of the disease (Aufderheide, Rodríguez-Martín 1998, Buikstra 1981, Morse 1978). Although convincing arguments have been offered and diagnostic criteria have been sharpened, some debate has been sustained because of the complexities involved.

More recently, molecular techniques have become available offering diagnostic criteria that bypass the difficulties of assessing skeletal response to the disease (Pérez-Pérez *et al.* 1995).

Work involving a joint project between the UCL Institute of Archaeology and the UCL Medical School's Department of Bacteriology has contributed to this knowledge, being the first to successfully extract and publish reports on the finding of bacterial DNA from ancient bones (Spigelman, Lemma 1993). This led to the isolation and amplification of a species-specific sequence from *Mycobacterium tuberculosis* (TB) in bones showing morphological evidence of tuberculosis. The PCR system for tuberculosis was based on the insertion sequence by Eisenach *et al.* (1990). The four bones containing this sequence originated from Europe, Turkey and pre-European contact Borneo, and ranged in age from 600 to 1700 AD. This first experiment may well have answered the question often asked whether Europeans brought tuberculosis to Asia – with a definite "no".

In related research, Rafi *et al.* (1994) successfully extracted and amplified the DNA of *Mycobacterium leprae* from human bone recovered from the Monastery of St. John the Baptist on the river Jordan, the site of a Christian massacre by Persians in 614 AD.

Also using techniques involving the polymerase chain reaction PCR, Salo *et al.* (1994) identified *Mycobacterium tuberculosis* DNA from a lung lesion of a mummy from southern Peru. This 40- to- 45 year-old female was recovered from a burial site in Chiribaya Alta and dated to between 1000 and 1300 AD. This work not only helped to demonstrate the applicability of this technique to palaeopathology, but effectively ended the debate regarding the pre-Columbian presence of tuberculosis in the New World. Ubaldi *et al.* (1998) summarize another recent research using molecular approaches to detect ancient DNA and report their own work on isolating bacterial DNA from Andean mummy tissue dating back to the 10–11 centuries AD.

In Israel, Donoghue *et al.* (1998) used molecular techniques to identify *Mycobacterium tuberculosis* in calcified pleura of 1,400-year-old remains, recovered from a Byzantine basilica in the Negev desert.

FORENSIC CASE

In 1992, human skeletal remains were submitted to the Smithsonian Institution through the Federal Bureau of Investigation for analysis from a law enforcement agency in the south-western area of the United States. The remains were found in an area considered to be a temperate semi-arid environment, at an elevation of about 1,150 m, with temperatures ranging from 40 to 60° F in winter and 90 to 100° F in summer. The remains were found shallowly buried in an eroded river bottom and were generally well preserved but lacked soft tissue and odour. The presence of associated plant roots, bleaching from apparent sun exposure, and surface alterations suggested a considerable time since death.

To clarify the antiquity of the remains, a bone sample was submitted for radiocarbon analysis to Beta Analytic Inc. of Miami, Florida, USA. Analysis indicated the individual was likely alive between 1670 and 1956 AD.

Analysis revealed that most bones and teeth were present, consistent with a single individual. The remains were complete except for a portion of the hyoid, both patellae, the bones of both feet and some hand bones. All teeth were present except the maxillary left third molar.

Female sex was suggested by general gracility and the morphology of the pelvis. In particular, female sex was suggested by a wide subpubic angle, wide pubis, and other indicators in the pubic area.

An age at death between 16 and 21 years was indicated by the extent of dental development and epiphyseal union. The apical root on the maxillary third molar was incompletely formed, the basilar synchrondrosis was fused but incomplete, and epiphyseal fusion was present on the clavicles and aspects of bones of the pelvis, knee, and wrist.

Pathological conditions included marked asymmetry in the posterior cranial area, and to a lesser extent, the bones of the face. The condition was sufficiently extreme to suggest a possible diagnosis of torticollis (wry-neck).

The dominant pathological condition, however, consisted of a large number of lesions distributed throughout the skeleton. Description of these lesions is as follows:

Cranium

A sharp-edged perforation, measuring 8 mm in diameter on the right coronal suture, 26 mm above pterion. The lesion is smooth walled, with a greater degree of erosion of the diploë than the inner or outer tables. No reactive bone was noted.

C1: Two coalescing, irregular, sharp-edged, deep, cavitating lesions are present on the left lateral transverse process, lateral to the foramen, on the dorsal aspect. Together, the lesions measure 4 × 5 mm. Slight new bone formation was noted.

C2: An irregular, sharp-edged perforation is present on the left side of the spinous process (*Figure 1*). On the lateral (external) surface, the perforation measures 5 × 8 mm; the size of the perforation on the inferior surface is 5 × 5 mm. Minimal reactive bone was noted. A sharp-edged, deep, cavitating lesion measuring 2 mm in diameter is present on the right inferior surface of the junction of the lamina and spinous process. No reactive bone is associated with this lesion.

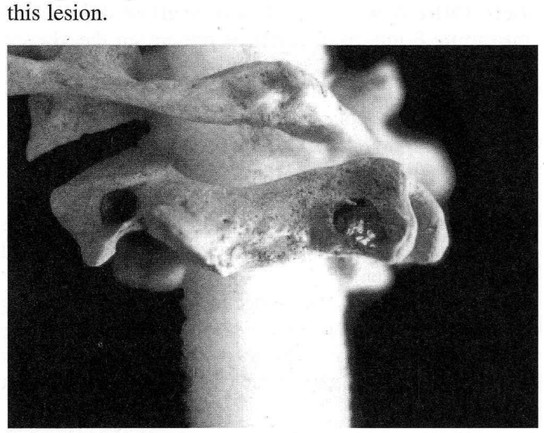

FIGURE 1. Irregular, sharp-edged perforation on spinous process of the second cervical vertebra.

C3: An irregular, shallow sharp-edged, cavitating lesion is present on the inferior aspect of the spinous process, measuring 4 × 5 mm in diameter. No reactive bone was noted; this may represent a postmortem artefact.

C4: An irregular, sharp-edged, cavitating lesion, measuring 2 × 6 mm, is present on a border of the left transverse process, superior surface. No reactive bone was noted.

T1 and T3: Each bone shows an area of sharp-edged, focal bone loss on the spinous process. No reactive bone was noted.

T7: A slight erosive area is present on the inferior surface of the right side of the centrum, near the vertebral canal, measuring 6 × 8 mm in size. No reactive bone was noted.

T8: An irregular, erosive area (*Figure 2*) is present on most of the right side of the centrum, measuring 15 × 22 mm. The area shows porosity, but no reactive bone.

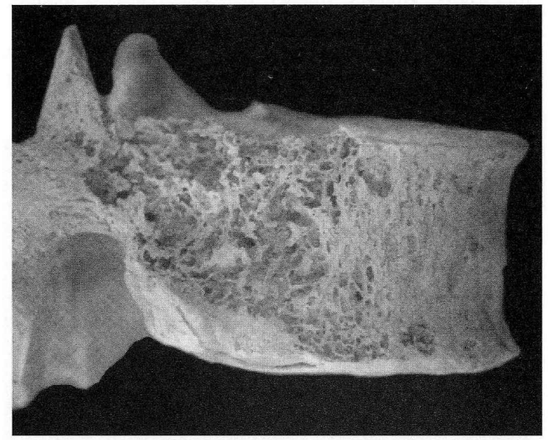

FIGURE 2. Irregular erosive area on the right side of the centrum of the 8th thoracic vertebra.

T9: An area of irregular, porotic bone formation is present on the ventral surface of the body, measuring 5 × 8 mm. In addition, there is a small, sharp-edged, deep, cavitating lesion on the right side of the spinous process measuring 2 mm in diameter. No reactive bone was noted in association with this second lesion.

T11: An area of unremodelled, fine, porous bone formation is present on most of the right side of the centrum.

L1: An area (6 × 18 mm) of slight, fine, porous reactive bone, both remodelled and unremodelled, is present on the right side of the centrum, just superior to the inferior rim.

L2: The superior aspect of the right side of the body is collapsed, primarily on the anterior portion. A moderate

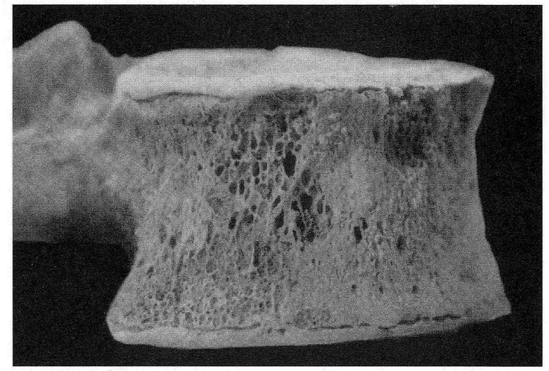

FIGURE 3. Erosive areas on the centrum of the 3rd lumbar vertebra.

amount of spicular bone formation is present over most of the non-articular surface of the centrum. This collapse likely would have led to an angulation of the superior spine slightly anterior and to the right.

L3: Approximately five porous, erosive areas are present on much of the anterior and right side of the centrum (*Figure 3*). Minimal spicular reactive bone is associated with this area.

L4: Moderately remodelled, porous new bone formation is present on both sides of the spinous process and the laminae (*Figure 4*).

FIGURE 4. Porous new bone formation on the spinous process and right lamina of the 4th lumbar vertebra.

Ribs

Except for the first ribs, all show areas of abnormal porosity on the visceral surface of the sternal ends, usually concentrated within an area 30 mm from the sternal border.

Left 1st: A sharp-edged, deep, cavitating lesion is present on the superior surface, measuring 4 mm in diameter, located 44 mm from the vertebral end. No reactive bone was noted.

Left 2nd: A sharp-edged, deep, cavitating lesion is present on the inferior surface, measuring 8 mm in diameter, and located 8 mm from the sternal end. Fine, slight, unremodelled bone was noted around the lesion, measuring about 10 × 19 mm. Plaque-like, remodelled bone is present on the visceral surface, beginning 5 mm from the vertebral border, in an area measuring 6 × 32 mm.

Left 3rd: Both remodelled and unremodelled new bone are present on the visceral surface, primarily in the area of the head, measuring 7 × 32 mm.

Left 4th: Both remodelled and unremodelled new bone deposits are present on the visceral surface, near the head (10 × 35 mm). Irregularly spaced areas along the costal groove and visceral surface of the sternal half are also involved.

Left 5th: A sharp-edged, deep, cavitating lesion is present on the inferior surface, measuring 7 mm in diameter and located 11 mm from the sternal end. Very fine, reactive bone and well-remodelled new bone are present along areas of the costal groove but are concentrated on both ends.

Left 6th: A sharp-edged, deep, cavitating lesion, measuring 3 mm in diameter, is present on the dorsal surface, between the head and the tubercle, 13 mm from the vertebral end, with no reactive bone associated. An area of well-remodelled, plaque-like bone formation is present on the visceral surface of most of the vertebral third. The costal groove area of the vertebral two-thirds shows irregularly scalloped, smooth-walled depressions, with areas of associated porous new bone.

Left 7th: The head shows destruction, but this may be due to post-mortem alteration of bone weakened by disease. Fine, partially remodelled new bone and irregular, well-remodelled deposits and shallow depressions are present over much of the visceral surface.

Left 8th: Four well-remodelled cavitations are present just superior to the costal groove, measuring 3 to 4 mm in diameter, located about 81 mm from the vertebral end. Fine, partially remodelled new bone is present over much of the visceral surface, along with well-remodelled, irregular deposits and shallow cavitations.

Left 9th: A series of apparently remodelled depressions is present on the visceral surface, the largest of which (the only deep depression) measures 9 mm in diameter, and is located 86 mm from the vertebral end. Well-remodelled bone formation is present over much of the visceral surface, along with some fine, porous, unremodelled bone deposits.

Left 10th: A well-remodelled, shallow depression, measuring 8 mm in diameter, is present on the visceral surface near the extreme sternal end. Remodelled new bone is present on the entire visceral surface with some fine, porous new bone concentrated on both ends.

Left 11th: Very slight, remodelled bone formation is present on the visceral surface, with unremodelled, fine, porous new bone deposits on the superior aspect of the bone.

Right 1st: A small porous cavitation is located on the superior surface, measuring 5 mm in diameter and located near the sternal end.

Right 2nd: A lytic, sharp-edged perforation, measuring 10 mm in diameter, is located near the midshaft on the lateral border (*Figure 5*). No reactive bone was noted, but the immediate area surrounding the lesion shows slight porosity.

FIGURE 5. A sharp-edged perforation on the lateral border of the right 2nd rib.

Right 3rd: A small, sharp-edged, deep, cavitating lesion, measuring 2 mm in diameter, is present on the lateral side of the rib, located 56 mm from the sternal end. No reactive bone was noted in association with the cavitation. The visceral side of the sternal aspect presents irregular porosity and a shallow cavitation measuring about 3 × 8 mm, 33 mm from the sternal border.

Right 4th: A small, sharp-edged, deep, cavitating lesion, measuring 2 mm in diameter, is present in the costal groove, located 84 mm from the sternal end. In addition, a shallow depression measuring 5 × 8 mm in diameter, is located in the costal groove, 20 mm from the sternal end. No reactive bone was noted.

Right 5th: A sharp-edged, deep, cavitating lesion is present in the costal groove, measuring 5 mm in diameter and located 61 mm from the vertebral end. A similar second lesion, measuring 3 mm in diameter, is located on the inferior border, 66 mm from the vertebral end. No reactive bone was noted.

Right 6th: Three sharp-edged deep cavitating lesions are located on the ventral surface. The first, measuring 3 mm in diameter, is located 18 mm from the sternal end. The second, measuring the same, is located 27 mm from the sternal end. The third is 1 mm in size, and located 33 mm from the sternal end. Remodelled bone is present irregularly around the area of the costal groove. Four well-remodelled depressions (three shallow and one moderately deep) are located in the costal groove. The first is 4 × 7 mm and located 74 mm from the vertebral end. The second is 3 × 7 mm and is located 90 mm from the vertebral end. The third measures 4 × 12 mm and is located 103 mm from the vertebral end. The fourth is 4 × 6 mm and is located 119 mm from the vertebral end.

Right 7th: On the lateral surface, a sharp-edged deep cavitating lesion measuring 3 × 8 mm is present. On the visceral surface (*Figure 6*), within the area of the costal groove, there are five roughly circular, smooth-edged depressions, as follows: 9 mm in diameter, 31 mm from the vertebral end (deep); 3 mm, 50 mm from the vertebral end (moderately deep; 13 mm, 82 mm from the vertebral end (very deep); 5 mm, 93 mm from the vertebral end (deep); 8 mm, 128 mm from the vertebral end (shallow). Remodelled and porous new bone covers much of the visceral surface.

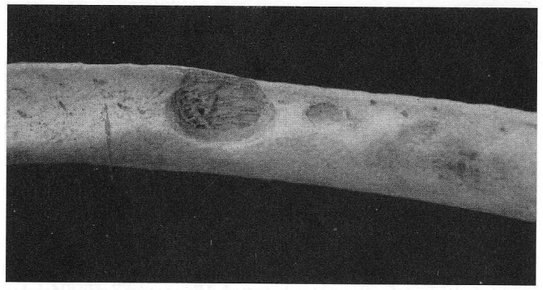

FIGURE 6. Smooth-edged depressions on the visceral surface of the right 7th rib.

Right 8th: Two depressions are located on the rim of the costal groove, one measuring 4 × 6 mm, 79 mm from the vertebral end (shallow), and one 5 × 6 mm, 89 mm from the vertebral end (moderately deep). The lesions appear to be remodelled. A slight amount of remodelled new bone is present on most of the visceral surface (*Figure 7*).

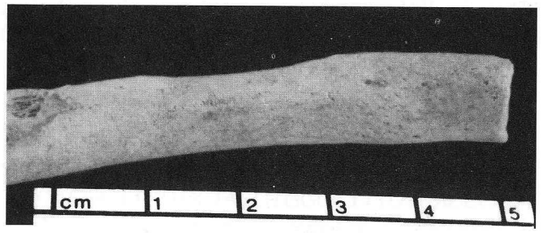

FIGURE 7. Remodelled new bone formation on the visceral surface (sternal end) of the right 8th rib.

Right 9th: Six deep, smooth-walled, well-remodelled depressions are present, all located in the area of the costal groove (*Figure 8*). The lesions measure as follows: 9 × 10 mm, 59 mm from the vertebral end; 8 × 9 mm, 62 mm from the vertebral end; 7 × 10 mm, 83 mm from the vertebral end; 7 × 8 mm, 98 mm from the vertebral end; 9 × 9 mm, 101 mm from the vertebral end; and 5 × 10 mm, 138 mm from the vertebral end. Remodelled new bone is present over most of the visceral surface (*Figure 9*).

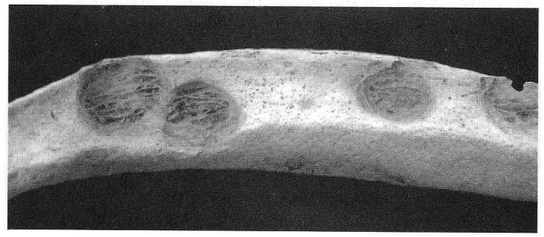

FIGURE 8. Smooth-walled cavitations on the visceral surface of the right 9th rib.

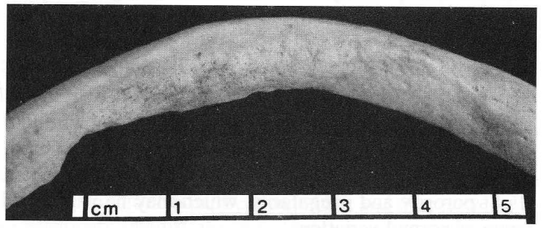

FIGURE 9. Remodelled new bone formation on the visceral surface of the right 9th rib.

Right 10th: Slight, remodelled new bone is present over most of the visceral surface.

Right 12th: A shallow depression, measuring 3 × 6 mm, is present in the area of the costal groove, 50 mm from the vertebral end.

Sternum
Areas of unusual porosity and bone formation are present over much of the sternum, especially on the dorsal aspect. It is unclear if this is pathological or within normal range.

Left clavicle
Three small (1 mm), sharp-edged, deep, cavitating lesions are present on the sternal articular end and the related metaphysis, with no associated bone formation.

Right clavicle
A small cavitation, measuring 3 × 4 mm, is present on the anterior surface, bordering the sternal end. No reactive bone was noted.

Right scapula
A 15 × 15 mm porous erosive lesion is present on the medial border (posterior surface) at the level of the acromial process. The lesion has a moth-eaten appearance, with no cavitation. A minimal amount of fine, porous, unremodelled new bone appears to be present just superior to the eroded area.

Left radius
An area of porosity and a small cavitation are present on the anterior surface of the area of the distal epiphyseal line and on the posterior aspect of the head. The first defect measures 4 mm in diameter; the second measures 7 mm. Note that the second lesion may represent post-mortem alteration.

Right radius
Irregularities are present on the distal epiphysis, near the epiphyseal line. Slight porosity is visible at three small sites along the line. This may represent post-mortem alteration.

Sacrum
Areas of fine porosity, with little remodelling or reactive bone, are present over much of the auricular areas. A shallow, cavitating lesion, measuring 3 mm in diameter, is present on the superior, right anterior surface of the ala of the first segment. The lesion is surrounded by a small amount of fine new bone, as well as an area of plaque-like bone located dorsally and medially to the perforations, measuring 6 × 11 mm. Other areas of the sacrum show slight porosity and irregularity, which may be within the range of normal variation.

Left innominate
New bone formation is visible on the ventral surface of the left pubis. It appears as fine, plaque-like, porous bone, in an area measuring 22 × 22 mm. Another area of bone formation is located just medially to the acetabulum, in the form of irregular, nodular bone deposits (*Figure 10*), measuring 12 × 20 mm. Also within the acetabulum, on the medial surface is an irregular cavitating lesion, partially smooth walled, and partially spicular in appearance, measuring 6 × 10 mm in size. This is located immediately posterior to the area of nodular deposits. On the ilium, an unremodelled area of erosion is present on the posterior auricular area. At least three ovoid sharp-edged, deep, cavitating lesions are also present on the iliac surface: a 5 × 7 mm lesion on the lateral side, 38 mm from the crest; a 6 mm lesion located 12 mm from the crest; and a 3 mm lesion located 5 mm from the iliac crest. Fine, porous, minimally remodelled reactive bone (*Figure 11*) is present around these three lesions.

FIGURE 10. Irregular nodular bone deposits near the acetabulum of the left innominate.

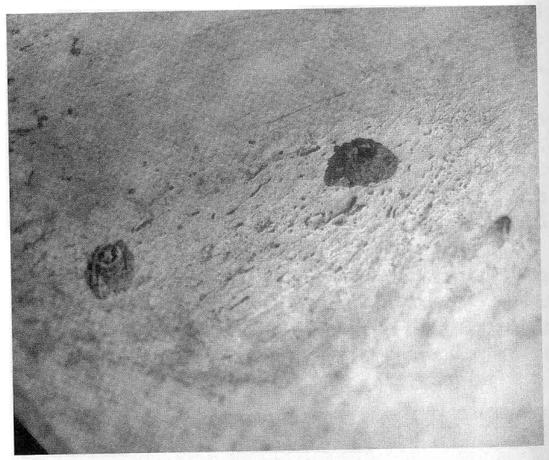

FIGURE 11. Fine, porous, minimally remodelled reactive bone associated with cavitating lesions on the left ilium.

Right innominate
On the right ilium, an area of unremodelled erosion is present in the sacro-iliac area, measuring about 39 × 50 mm. At least four sharp-edged, deep, cavitating lesions are present on the ilium: a 4 mm defect in the postauricular area; a 4 mm perforation located 17 mm anterior to the auricular area, 33 mm from the iliac crest; an 8 mm defect on the posterior inferior border of the iliac crest; and a 3 mm lesion is located on the medial ilium 48 mm from the anterior superior iliac spine. This 3 mm lesion nearly penetrates to the lateral surface, which displays an elevated area (5 × 7 mm) of new bone formation. The first two lesions show no reactive bone in association on the medial surface; the third shows a minimal amount of reactive bone over an area measuring 26 × 41 mm. This reactive bone is mostly fine and porous with some nodular formations. Remodelling is minimal. Note that an area of fine bone deposits measuring about 21 × 39 mm is present on the lateral surface in the area of the perforation described above. An area of coarse, spicular bone (measuring about 23 × 45 mm) is located just posterior to the acetabulum.

Right femur
A deposit of well-remodelled, periosteal new bone is present over most of the medial shaft. A porous, fine bone deposit is located 21 mm below the lesser trochanter, measuring 8 × 18 mm in size. The area shows a curvilinear vascular track in its center. Little remodelling is present associated with this lesion. A 3 × 4 mm sharp-edged, deep, cavitating lesion is present on the lateral/posterior surface between the lesser and greater trochanter. This lesion shows no evidence of remodelling.

The overall morphology and pattern of these lesions were strongly suggestive of tuberculosis. However, due to the difficulties of diagnosis from skeletal evidence alone, diseases of fungal origin or even others could not be entirely ruled out.

Because of the uncertainties of diagnosis from skeletal evidence alone, a sample of bone was removed for molecular study. A section of the right seventh rib displaying pathological alteration was utilized for this purpose. *Mycobacterium tuberculosis* DNA was isolated and positively identified from the sample through the use of nested PCR based on the 123 base pair (bp) sequence of IS6110 presented by Eisenach *et al.* (1990).

The DNA extraction methods were based on cell lysis with guanidium thiocyanate, and the direct absorption of DNA to a fine silica suspension (Donoghue *et al.* in press). This was followed by washing and DNA elution. An extended time was allowed for cell lysis, as preliminary work with mycobacterial cultures shows that this was necessary for reliable DNA extraction. Extraction controls containing no sample were always included in the procedure.

Nested PCR was used to detect *M. tuberculosis*-complex-specific DNA. The primers and basic method were described by Taylor *et al.* (1996). The target for DNA amplification was the repetitive element in the *M. tuberculosis* genome known as the insertion sequence IS6110. This element is normally present in multiple copies in *M. tuberculosis* isolates and the first pair of primers (P1 and P2) amplify a 123 bp region of IS6110 (Eisenach *et al.* 1990). The second set of primers, IS-3 and IS-4, bind internally with some overlap to P1 and P2 and amplify a 92 bp product. Nested PCR is exquisitely sensitive, so stringent precautions were necessary to avoid cross-contamination.

There was no visible product from positive control of experimental samples after the first stage of amplification, although a faint band of 123 bp was visible with the positive control.

After nested PCR, a band of the expected size (92 bp) was visible.

The product was sequenced using the primer IS-3; a sequence of 72 bases was obtained which confirmed the presence of tuberculosis:
GGCTGTGGGTAGCAGACCTCACCTATGTGTCCACCTG
GGCAGGGTTCG CCTACGTGGCCTTTGTCACCGGA.

This identical sequence is found in 25 sequences of *M. tuberculosis* IS6100 held in the gene data bank. On comparing the sequence with those published, it was clear that the sequence was obtained starting only two bases downstream from the sequencing primer, and extended to the end of the expected DNA template.

DISCUSSION

Molecular analysis confirmed the diagnostic of tuberculosis suggested by the pattern and morphology of skeletal lesions. The roughly circular cavitating lesions, minimal bone response, slightly sclerotic margins of some lesions, vertebral centra collapse, and site selection for areas of high blood content are all indicative of skeletal tuberculosis. Involvement of the neural arches, transverse processes, and spinous processes of the vertebrae, especially the cervicals, is unusual for tuberculosis and more suggestive of coccidioidomycosis. Although this young woman suffered from advanced skeletal tuberculosis, other accompanying diseases cannot be ruled out.

CONCLUSION

To our knowledge, this case represents the first example of how molecular techniques can be used to positively identify a disease organism that affected a human host in a forensic case. This information assists the investigation of the case. Although this case appears to be of considerable antiquity, in other forensic cases such information might lead investigators to medical treatment and thus the means to positively identify the individual.

This case also presents an example of how molecular techniques can be used to confirm a disease diagnosis suggested by skeletal lesions. This confirmed case documents the extent and diversity of skeletal lesions within an individual suffering from tuberculosis.

REFERENCES

ALLISON M. J., MENDOZA D., PEZZIA A., 1973: Documentation of a case of tuberculosis in pre-Columbian America. *American Review of Respiratory Disease* 107: 985–991.

AUFDERHEIDE A. C., RODRÍGUEZ-MARTÍN C., 1998: *The Cambridge Encyclopaedia of Human Paleopathology.* University Press, Cambridge.

BUIKSTRA J. E. (Ed.), 1981: *Prehistoric Tuberculosis in the Americas.* Northwestern University Archaeological program, Evanston (IL).

DALTON H. P., ALLISON M. J., PEZZIA A., 1976: The documentation of communicable diseases in Peruvian mummies. *MCV Quarterly* 12,2: 43–48.

DONOGHUE H. D., SPIGELMAN M., ZIAS J., GERNAEY-CHILD A. M., MINNIKIN D. E., 1998: Mycobacterium tuberculosis complex DNA in calcified pleura from remains 1400 years old. *Letters in Applied Microbiology* 27: 265–269.

DONOGHUE H. D., UBELAKER D. H., SPIGELMAN M. (in print): The case of paleomicrobiological techniques in a current forensic case. In: G.Palfi, W. Dutour, J. Deak, I. Hutas (Eds.): *The Past and Present of Tuberculosis: Biology, Evolution, Diagnosis, History and Paleoepidemiology of TB*. Szeged, Hungary.

EISENACH, K. D., CAVE M. D., BATES J. H., CRAWFORD J. T., 1990: Polymerase chain reaction amplification of a repetitive DNA sequence specific for Mycobacterium tuberculosis. *Journal of Infectious Diseases* 161: 977–981.

HRDLIČKA A., 1909: Tuberculosis among certain Indian tribes. *Bureau of American Ethnology Bulletin* 42: 1–48.

KELLEY M. A., MICOZZI M. S., 1984: Rib lesions and chronic pulmonary tuberculosis. *Amer. J. of Phys. Anthrop.* 65: 381–386.

KELLEY M. A., MURPHY S. P., LEVESQUE D. R., SLEDZIK P. S., 1994: Respiratory disease among protohistoric and early historic Plains Indians. In: D. W. Owsley, R. L. Jantz (Eds.): *Skeletal Biology in the Great Plains.* Pp.123–130. Smithsonian Institution Press, Washington (DC).

MORSE D., 1978: Ancient disease in the Midwest (2nd ed.). *Illinois State Museum Report of Investigations* 15.

ORTNER D. J., PUTSCHAR W. G. J., 1981: *Identification of Pathological Conditions in Human Skeletal Remains.* Smithsonian Contributions to Anthropology 28. Smithsonian Institution Press, Washington (DC).

PÉREZ-PÉREZ A., GIRBAU E., LALUEZA C., 1995: Ancient DNA analysis: Detection of disease and mt-DNA variability. *Proceedings of the IXth European Meeting of the Paleopathology Association* pp. 273–278. Museu d'Arqueologia de Catalunya, Barcelona.

RAFI A., SPIGELMAN M., STANFORD J., LEMMA E., DONOGHUE H., ZIAS J., 1994: DNA of Mycobacterium leprae detected by PCR in ancient bone. *Internat. J. of Osteoarcheology* 4: 287–290.

SALO W. S., AUFDERHEIDE A. C., BUIKSTRA J., HOLCOMB T. A., 1994: Identification of Mycobacterium tuberculosis DNA in a pre-Columbian Peruvian mummy. *Proc. Natl. Acad. Sci. USA* 91: 2091–2094.

SPIEGELMAN M., LEMMA E., 1993: The use of the polymerase chain reaction to detect Mycobacterium tuberculosis in ancient skeletons. *Internat. J. of Osteoarcheology* 3: 137–143.

STEINBOCK R. T., 1976: *Paleopathological Diagnosis and Interpretation.* Charles C. Thomas, Springfield (IL).

TAYLOR G. M., CROSSEY M., SALDANHA J., WALDRON T., 1996: Mycobacterium tuberculosis identified in Medieval human skeletal remains using polymerase chain reaction. *J. Archeol. Sci.* 23:789–798.

UBALDI M., LUCIANI S., MAROTA I., FORNACIARI G., CANO R. J., ROLLO F., 1998: Sequence analysis of bacterial DNA in the colon of an Andean mummy. *Amer. J. of Phys. Anthrop.* 107: 285–295.

Douglas H. Ubelaker
Erica B. Jones
Department of Anthropology/MRC 112
National Museum of Natural History
Smithsonian Institution
Washington, DC 20560
USA

Helen D. Donoghue
Mark Spigelman
Bacteriology Department
Royal Free and University College School of Medicine
Windeyer Institute of Medical Sciences
The Windeyer Building
46 Cleveland Street
London W1P DP
UK